archives
of thermodynamics
Vol. **32**(2011), No. 2, 3–20
DOI: 10.2478/v10173-011-0006-4

Efficiency optimization of a closed indirectly fired gas turbine cycle working under two variable--temperature heat reservoirs

ZHESHU MA[1*]
JIEER WU[2]

[1] Department of Power Engineering, Jiangsu University of Science and Technology, Zhenjiang, 212003, China

[2] School of Mathematics & Physics, Jiangsu University of Science and Technology, Zhenjiang, 212003, China

Abstract Indirectly or externally fired gas turbines (IFGT or EFGT) are interesting technologies under development for small and medium scale combined heat and power (CHP) supplies in combination with micro gas turbine technologies. The emphasis is primarily on the utilization of the waste heat from the turbine in a recuperative process and the possibility of burning biomass even "dirty" fuel by employing a high temperature heat exchanger (HTHE) to avoid the combustion gases passing through the turbine. In this paper, finite time thermodynamics is employed in the performance analysis of a class of irreversible closed IFGT cycles coupled to variable temperature heat reservoirs. Based on the derived analytical formulae for the dimensionless power output and efficiency, the efficiency optimization is performed in two aspects. The first is to search the optimum heat conductance distribution corresponding to the efficiency optimization among the hot- and cold-side of the heat reservoirs and the high temperature heat exchangers for a fixed total heat exchanger inventory. The second is to search the optimum thermal capacitance rate matching corresponding to the maximum efficiency between the working fluid and the high-temperature heat reservoir for a fixed ratio of the thermal capacitance rates of the two heat reservoirs. The influences of some design parameters on the optimum heat conductance distribution, the optimum thermal capacitance rate matching

*Corresponding author. E-mail address: mazheshu@126.coml

and the maximum power output, which include the inlet temperature ratio of the two heat reservoirs, the efficiencies of the compressor and the gas turbine, and the total pressure recovery coefficient, are provided by numerical examples. The power plant configuration under optimized operation condition leads to a smaller size, including the compressor, turbine, two heat reservoirs and the HTHE.

Keywords: Indirectly fired gas turbine, Bioenergy technology; High temperature heat exchanger; Finite time thermodynamics; Cycle performance

Nomenclature

C_{wf}	—	thermal capacitance rate of working fluid, kJ/(s K)
C_H		thermal capacitance rate of high-temperature (hot-side) heat reservoir, kJ/(s K)
C_L	—	thermal capacitance rate of cold-side heat reservoir, kJ/(s K)
$C_{H\,\min}$	—	smaller of C_H and C_{wf}, kJ/(s K)
$C_{H\,\max}$	—	larger of C_H and C_{wf}, kJ/(s K)
$C_{L\,\min}$	—	smaller of C_L and C_{wf}, kJ/(s K)
$C_{L\,\max}$	—	larger of C_L and C_{wf}, kJ/(s K)
c_p	—	specific heat, kJ/(kg K)
D	—	total pressure recovery coefficient
E_H	—	effectivenesses of hot-side heat exchanger
E_L	—	effectivenesses of cold-side heat exchanger
E_{HE}	—	effectiveness of high temperature heat exchanger
k	—	adiabatic exponent (specific heat ratio)
$\dot{m}$	—	mass flow, kg/s
N_H	—	number of heat transfer units of hot-side heat exchanger
N_L	—	number of heat transfer units of cold-side heat exchanger
N_{HE}	—	number of heat transfer units of high temperature heat exchanger
p_i	—	pressure of state$i$, Pa
P	—	power output of indirectly fired gas turbine cycle
P^*	—	dimensionless power output of indirectly fired gas turbine cycle
$\dot{Q}_H$	—	rate of heat supplied to high-temperature reservoir
$\dot{Q}_L$	—	rate of heat removed to low-temperature reservoir
$\dot{Q}_R$	—	rate of heat exchanged in HTHE
T_i	—	temperature of state i, K
T_{Lin}	—	inlet temperature of cold-side heat reservoir, K
U_H	—	heat conductance of high-temperature heat reservoir, W/(m^{2}K)
U_L	—	heat conductance of low-temperature heat reservoir, W/(m^{2}K)
U_{HE}	—	heat conductance of high-temperature heat reservoir, W/(m^{2}K)
U_T	—	total heat exchanger inventory
u_H	—	heat conductance distribution of hot-side heat reservoir
u_L	—	heat conductance distribution of cold-side heat reservoir
x	—	isentropic temperature ratio

Greek symbols

θ_i	—	dimensionless temperature of state i
θ_{Tin}	—	cycle heat reservoir inlet temperature ratio
η	—	cycle efficiency of indirectly fired gas turbine cycle
η_c	—	isentropic efficiency of the compressor
η_t	—	gas turbine's isentropic efficiency
η_{HE}	—	efficiency of the high temperature heat exchanger
$\eta_{\max}$	—	optimum cycle efficiency
π_c	—	cycle pressure ratio
$\pi_{c,opt}$	—	pressure ratio corresponding to maximum cycle efficiency

Subscripts

in	—	inlet
out	—	outlet

1 Introduction

Classical thermodynamics is typically used for analyzing energy systems or components, and it basically considers equilibrium states and generally slow rates that typically result in infinite time processes; however, finite work divided by infinite times produces zero power, thus no practical applications for realistic power production arise in consideration of concepts and cycles in classical thermodynamics. Modeling of real processes in which the working fluid passes through hardware and/or components of finite size in finite-time periods involves irreversibilities which necessitate considerations regarding their quantification with time-size constraints becoming important. Finite-time thermodynamics (FTT) or entropy generation minimization (EGM) concepts provide an approach to quantify cycles and plant component irreversibilities and ultimately can provide a more rationally based prescription applicable to engineering design and development processes. Since the pioneering work of Novikov [1], Chambadal [2], and Curzon and Ahlborn [3], FTT has been used progressively in cycle and power plant performance analyses and a large amount of information has been published in this field [4,5].

In recent years, renewable energy utilization has grown rapidly. Electricity generated by utilizing renewable energy sources occupied 19% of the world electricity production in 2005 [6]. The state-of-the-art regarding renewable energy sources include large hydropower and other sources such as wind, biomass, solar, geothermal, and small hydros. However, related energy conversion technologies should for optimum benefit combine high conversion-efficiencies with low emissions leading to especially careful

considerations for the widely publicized CO_2 emission levels. As a consequence, accurate design methods and optimal device energy performance for these novel conversion technologies assume a most significant activity, since, commercial applications or even their demonstrations are costly and time-consuming including a high risk of failure, e.g., UK's unsuccessful "flagship" Project Arable Biomass Renewable Energy (ARBRE) [7]. Thus, the need to develop both scientific and reasonable engineering criteria to define objective functions and to perform the required optimization on these functions becomes apparent. The following criteria combine a number of conflicting but nevertheless important variables contributing to the engineering task in hand: maximum power, minimum entropy generation, maximum power density, first law efficiency, ecological criterion, maximum profit, and second law efficiency. These different approaches are taken according to the specific needs for the desired application; however, on consideration of certain conditions some of the above criteria are shown to be equivalent [8]. Many researchers have applied the above mentioned objective functions to different processes.

As distinct from the mature/advanced modern energy-conversion technologies including internal combustion engines and ordinary gas turbines which demand clean fuels as combustion gases (working fluid) are in direct contact with the moving parts of the machine, indirectly fired gas turbine (IFGT) cycles employ indirect combustion systems thereby separating the combustion process and thermodynamic conversion process. This practice allows utilizations of "dirty" fuels including biomass and waste fuel as practical possibilities. Recently, IFGT cycles have also involved a class of state-of-the-art promising research undertakings in a variety of applications internationally. In addition to the conventional coal-fired steam cycle plants and Stirling engines, indirectly or externally-fired gas-turbine (IFGT or EFGT) also appear as a novel technology item under development for small and medium scale combined heat and power (CHP) applications in combination with micro gas turbine technologies [9]. The most attractive advantage of IFGT units is that they open new and exciting avenues to utilize biomass for CHP and contribute to reducing greenhouse-gas emissions while offering engineering possibilities for higher conversion efficiency. Up to now, studies of externally fired gas turbines have been performed by a number of different research organizations and power equipment manufacturers. Currently, available analyses concentrate on various cycle configurations to attain high conversion efficiencies [10–27], including different types of furnace arrange-

ments [13–15], and the development of possible high-temperature heat exchangers [10–14]. In addition, several excellent review papers and reports on IFGT applications are available [15–17].

Based on various finite time thermodynamic formulae derived for a real irreversible closed cycle working between two finite heat reservoirs while incorporating in addition various resistances for heat transfer, this paper aims to optimize the dimensionless cycle power output using the theory of thermodynamic optimization by searching for the optimum heat conductance distribution among the three heat exchangers (the hot-side and cold-side heat reservoirs, and the high temperature heat exchanger) for a fixed total heat exchanger inventory. In the analysis, the heat resistance losses in the three heat exchangers, the irreversible compression and expansion losses in the compressors and the turbine, and the pressure drop loss at the heater, cooler and regenerator as well as in the piping, are taken into account. The effects of some cycle parameters on the cycle optimum performance have been derived numerically and summarized by illustrations.

2 Model cycle and analytical relation

The schematic and T-S diagrams of the closed IFGT cycles studied are shown in Figs. 1 and 2, respectively. The working air enters the compressor at state 1 and is nonisentropically compressed to state 2. After state 2 (ideally to the state 2s), the air leaving the compressor enters the high temperature heat exchanger (HTHE) and is heated to state 3 via the high temperature combusted biomass gas flow. Then the heated air enters the gas turbine and expands nonisentropically to state 4 (ideally to state 4s). After leaving the gas turbine, the still hot air enters the combustion chamber and takes part in the combustion process with biomass fuel to the highest temperature point of the cycle, i.e., state 5. The hot gas then exits the combustion chamber and enters the HTHE, where it adds heat to the air and in return is cooled to state 6 at constant pressure. Finally, the cycle is completed by cooling the gas to the initial state. In Fig. 2, the process 1-2s is an isentropic compression and 1-2 takes into account the nonisentropic nature of a real compressor; the process 3-4s is an isentropic expansion while 3-4 signifies a real nonisentropic expansion in a real turbine.

In order to analyze the efficiency characteristics of the IFGT cycle under consideration, following assumptions are made for the one dimensional ideal gas steady flow and application conservation of energy principle to each

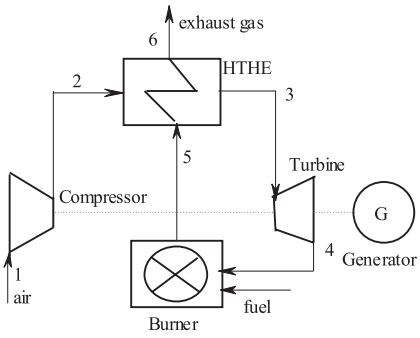

Figure 1. Schematic diagram of the IFGT cycle.

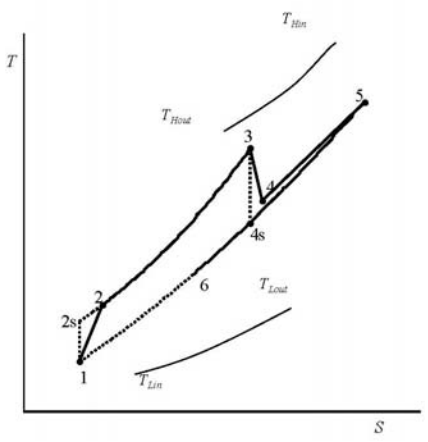

Figure 2. T–S diagram of the IFGT cycle.

component:

(i) The working fluids (air and combustion gases) are ideal gases and each possesses constant specific heat. The working fluids flow through the system in a one-dimensional quasistatic-state fashion.

(ii) The compression process 1-2 and expansion process (4-5) are adiabatic and irreversible. The deviations from the isentropic processes are accounted for by the isentropic efficiencies. The gas turbine's isentropic efficiency η_t, gives the ratio of the actual expansion process producing power to the isentropic one. The isentropic efficiency of the compressor η_c, is defined as the ratio of the power requirement during the isentropic compression to that of the actual compression. Efficiencies η_t and η_c have the values between zero and unity:

$$\eta_t = \frac{T_3 - T_4}{T_3 - T_{4s}} \,, \tag{1}$$

$$\eta_c = \frac{T_{2s} - T_1}{T_2 - T_1} \,. \tag{2}$$

(iii) The heat transfer in the real high temperature heat exchanger (HTHE) is described by using the HTHE efficiency η_{HE}. This efficiency is defined as follows

$$\eta_{HE} = \frac{T_3 - T_2}{T_5 - T_6} \,, \tag{3}$$

which is the ratio of the actual heat transfer process 2-3 to the maximum idealistic amount of heat transfer (5-6). The value of η_{HE} varies from 0 to 1.

(iv) The cycle has a pressure ratio, which is the ratio of the maximum pressure of the cycle obtained at the compressor exit (state 2) to the minimum pressure of the cycle at the turbine exit which corresponds to the compressor inlet (state 1), i.e.,

$$\pi_c = \frac{p_2}{p_1} \,. \tag{4}$$

(v) The pressure drop in the flow piping is reflected by using a total pressure recovery coefficient, that is:

$$D = 1 - \frac{\Delta p}{p} \,, \tag{5}$$

$$\frac{p_3}{p_4} = D\,\frac{p_2}{p_1} \,, \tag{6}$$

where p denotes pressure. The working fluid is an ideal gas with a constant thermal capacitance rate C_{wf} ($C_{wf} = \dot{m}c_p$, mass flow times the specific heat). The high-temperature (hot-side) heat reservoir is assumed to have a finite thermal capacitance rate C_H. The inlet and outlet temperatures of the heating fluid are T_{Hin} and T_{Hout}, respectively. The low-temperature (cold-side) heat reservoir is also assumed to have a finite thermal capacitance rate C_L and the inlet and outlet temperatures of the cooling fluid are T_{Lin} and T_{Lout}, respectively. All heat exchangers, including the high temperature heat exchanger, are assumed to be counter-flow heat exchangers with constant heat conductances U_H, U_L and U_R. The heat conductance is defined as the product of the overall heat transfer coefficient and the heat transfer surface area of the heat exchanger. According to the principles of heat transfer and thermodynamics, the rates at which heat is supplied, rejected and transferred in the high temperature heat exchanger are given by the following expressions:

$$\dot{Q}_H = \dot{Q}_{4-5} = U_H \frac{(T_{Hin} - T_5) - (T_{Hout} - T_4)}{\ln\left[(T_{Hin} - T_5)\,/\,(T_{Hout} - T_4)\right]} = C_H\,(T_{Hin} - T_{Hout}) \,, \tag{7}$$

$$\dot{Q}_L = \dot{Q}_{6-1} = U_L \frac{(T_6 - T_{Lout}) - (T_1 - T_{Lin})}{\ln\left[(T_6 - T_{Lout})\,/\,(T_1 - T_{Lin})\right]} = C_L\,(T_{Lout} - T_{Lin}) \,, \tag{8}$$

$$\dot{Q}_H = C_{wf}\left(T_5 - T_4\right) \ , \tag{9}$$

$$\dot{Q}_L = C_{wf}\left(T_6 - T_1\right) \ , \tag{10}$$

$$\dot{Q}_R = C_{wf}\left(T_5 - T_6\right) = C_{wf}\left(T_3 - T_2\right) \ , \tag{11}$$

$$\dot{Q}_H = C_{H\,\min} E_H \left(T_{Hin} - T_4\right) \ , \tag{12}$$

$$\dot{Q}_L = C_{L\,\min} E_L \left(T_6 - T_{Lin}\right) \ , \tag{13}$$

$$\dot{Q}_R = C_{wf} E_{HE} \left(T_5 - T_2\right) \ , \tag{14}$$

where E_H and E_L denote the effectiveness of the hot-side and cold-side heat exchangers and E_{HE} is the effectiveness of the high temperature heat exchangers.

The effectivenesses of the heat exchangers are defined as:

$$E_H = \frac{1 - \exp\left[-N_H\left(1 - \dfrac{C_{H\,\min}}{C_{H\,\max}}\right)\right]}{1 - \dfrac{C_{H\,\min}}{C_{H\,\max}} \exp\left[-N_H\left(1 - \dfrac{C_{H\,\min}}{C_{H\,\max}}\right)\right]} \ , \tag{15}$$

$$E_L = \frac{1 - \exp\left[-N_L\left(1 - \dfrac{C_{L\,\min}}{C_{L\,\max}}\right)\right]}{1 - \dfrac{C_{L\,\min}}{C_{L\,\max}} \exp\left[-N_L\left(1 - \dfrac{C_{L\,\min}}{C_{L\,\max}}\right)\right]} \ , \tag{16}$$

$$E_{HE} = \frac{N_{HE}}{N_{HE} + 1} \ , \tag{17}$$

where $C_{H\,\min}$ and $C_{H\,\max}$ are the smaller and the larger of the two capacitance rates C_H and C_{wf}, while $C_{L\,\min}$ and $C_{L\,\max}$ are the smaller and the larger of the two capacitance rates C_L and C_{wf}:

$$C_{H\,\min} = \min\left\{C_H, C_{wf}\right\} \ , \tag{18}$$

$$C_{H\,\max} = \max\left\{C_H, C_{wf}\right\} \ , \tag{19}$$

$$C_{L\,\min} = \min\left\{C_L, C_{wf}\right\} \ , \tag{20}$$

$$C_{L\,\max} = \max\left\{C_L, C_{wf}\right\} \ . \tag{21}$$

Here N_H and N_L are the numbers of heat transfer units of the hot-side and cold-side heat exchangers, while N_{HE} is the number of heat transfer units of the high temperature heat exchanger. The heat transfer units are

based on the minimum thermal capacitance rates and can be expressed in the following expressions:

$$N_H = \frac{U_H}{C_{H\min}}, \quad N_L = \frac{U_L}{C_{L\min}}, \quad N_R = \frac{U_R}{C_{wf}} \,. \tag{22}$$

Define x as the isentropic temperature ratio in the compressor. According to the knowledge of thermodynamics, one can obtain:

$$x = \frac{T_{2s}}{T_1} = \left(\frac{p_2}{p_1}\right)^m = \pi_c^m \,, \tag{23}$$

where $m = \frac{k-1}{k}$ and k is adiabatic exponent (ratio of respective specific heats).

According to the definition of total pressure recovery coefficient, one can obtain the isentropic temperature ratio in the gas turbine:

$$\frac{T_3}{T_{4s}} = \left(\frac{p_3}{p_4}\right)^m = (\pi D)^m = xD^m \,. \tag{24}$$

Define dimensionless temperature:

$$\theta_i = T_i / T_{Lin} \,. \tag{25}$$

Thus the dimensionless power output and cycle efficiency of the IFGT cycle can be derived:

$$\begin{aligned}
P^* &= \frac{P}{C_L T_{Lin}} = \frac{\dot{Q}_H - \dot{Q}_L}{C_L T_{Lin}} \\
&= \frac{C_{H\min}}{C_{wf}} E_H \left(\theta_{Hin} - \theta_4\right) - \frac{C_{L\min}}{C_{wf}} E_L \left(\theta_6 - 1\right) \\
&= \left(C_{H\min}\frac{E_L}{C_{wf}}\right)\theta_{Hin} - \left(C_{H\min}\frac{E_L}{C_{wf}}\right) \times \\
&\quad \times \Big\{ \left[(c - cd)\left(2E_{HE} - 1\right) - E_{HE} \right] b\theta_{Hin} + \left(E_{HE} - 1\right) cd \Big\} \Big/ \\
&\quad \Big/ \Big\{ \left[a + E_{HE}\left(b - 1\right) \right] \left(c - cd - 1\right) + \\
&\quad + \left(a + b - 1\right)\left(c - cd\right)\left(E_{HE} - 1\right) \Big\} - \left(C_{L\min}\frac{E_L}{C_{wf}}\right) \times \\
&\quad \times \Big\{ c\left(a + b - 1\right)\left(1 - E_{HE}\right) + \left(1 - c\right)\left[a + E_{HE}\left(b - 1\right) \right] + \\
&\quad + ab\left(E_{HE} - 1\right)\theta_{Hin} \Big\} \Big/ \Big\{ \left[a + E_{HE}\left(b - 1\right) \right] \left(c - cd - 1\right) + \\
&\quad + \left(a + b - 1\right)\left(c - cd\right)\left(E_{HE} - 1\right) \Big\} \,,
\end{aligned} \tag{26}$$

$$\begin{aligned}
\eta &= \frac{P}{\dot{Q}_H} = 1 - \frac{\dot{Q}_L}{\dot{Q}_H} \\
&= 1 - \frac{C_{L\min}E_L}{C_{H\min}E_H} \times \frac{\theta_6 - 1}{\theta_{Hin} - \theta_4} \\
&= 1 - (C_{L\min}E_L)/(C_{H\min}E_H) \times \Big\{ c\,(a+b-1)\,(1-E_{HE}) + \\
&\quad + (1-c)\left[a + E_{HE}\,(b-1)\right] + ab\,(E_{HE}-1)\,\theta_{Hin} \Big\} \Big/ \\
&\quad \Big/ \Big\{ \left[a + E_{HE}\,(b-1)\right](c - cd - 1)\,\theta_{Hin} + \\
&\quad + (a+b-1)\,(c-cd)\,(E_{HE}-1)\,\theta_{Hin} + \\
&\quad + \left[(c-cd)\,(2E_{HE}-1) - E_{HE}\right] b\,\theta_{Hin} + \\
&\quad + (1-E_{HE})\,cd \Big\} \,, \qquad (27)
\end{aligned}$$

where

$$a = 1/\left(1 - \eta_t + x^{-1}D^{-m}\eta_t\right) \,, \qquad (28)$$

$$b = \frac{C_{H\min}E_H}{C_{wf}} \,, \qquad (29)$$

$$c = \frac{\eta_c + x - 1}{\eta_c} \,, \qquad (30)$$

$$d = \frac{C_{L\min}E_L}{C_{wf}} \,. \qquad (31)$$

Equations (26) and (27) indicate that the dimensionless power output P^* and cycle efficiency η of the specific IFGT cycle considered are complicated functions of the isentropic efficiencies of the gas turbine η_t and the compressor η_c, the total pressure recovery coefficient D, the cycle pressure ratio π_c, the cycle heat reservoir inlet temperature ratio θ_{Tin}, heat transfer effectiveness of both the hot-side heat reservoir E_H, and the cold-side heat reservoir E_L, heat transfer effectiveness of the regenerator E_{HE}, thermal capacitance rates of both the hot-side C_H, and the cold-side heat reservoir C_L and thermal capacitance rate of the working fluid C_{wf}.

3 Optimum distribution of heat conductance

For the fixed heat conductances U_H, U_L and U_{HE}, Eq. (27) shows that there exists an optimum pressure ratio $\pi_{c,opt}$ which leads to maximum cycle efficiency. In the practical design, U_H, U_L and U_{HE} are interchangeable. For a fixed pressure ratio, there exists a pair of optimum distributions

among the heat conductances of hot- and cold-side heat reservoirs and the high temperature heat exchanger for a fixed total heat exchanger inventory, leading to optimum cycle efficiency $\eta_{\max}$. The optimum pressure ratio $\pi_{c,opt}$ and a pair of optimum distributions lead to the maximum optimum (double-maximum) cycle efficiency $\eta_{\max,\max}$. They may be determined using numerical calculations.

For a fixed total heat exchanger inventory U_T, i.e., for the constraint

$$U_H + U_L + U_{HE} = U_T \ , \tag{32}$$

defining the heat conductance distribution of hot-side heat reservoir u_H, and the heat conductance distribution of cold-side heat reservoir, u_L, as

$$u_H = U_H/U_T \ , \tag{33}$$

$$u_L = U_L/U_T \ , \tag{34}$$

leads to

$$U_H = u_H U_T \ , \tag{35}$$

$$U_L = u_L U_T \ , \tag{36}$$

$$U_{HE} = (1 - u_H - u_L)\, U_T \ . \tag{37}$$

The efficiency optimization is performed via a numerical calculation. In the calculation, the respective parameters are set to $C_H = 2.0$ kW/K, $C_L = 2.0$ kW/K, $C_{wf} = 1.0$ kW/K and $k = 1.4$. In the numerical calculation, additionally the following numerical constraints should be satisfied:

$$0 < u_H < 1 \ , \tag{38}$$

$$0 < u_L < 1 \ , \tag{39}$$

$$0 < u_H + u_L < 1 \ . \tag{40}$$

The influence of the cycle inlet temperature ratio (θ_{Hin}) for the two heat reservoirs on the optimum cycle efficiency ($\eta_{\max}$) versus pressure ratio (π_c) with $U_T = 7.0$ kW/K, $\eta_c = 0.85$, $\eta_t = 0.85$ and $D = 0.93$ is shown in Fig. 3. The corresponding optimum heat conductance distributions ($u_{H,opt}$ and $u_{L,opt}$) and dimensionless power under optimal cycle efficiency condition ($P^*_{\eta,\max}$) are shown in Figs. 4, 5 and 6.

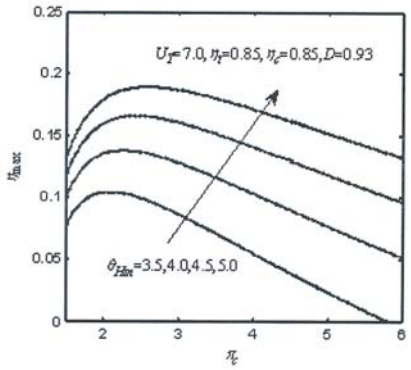

Figure 3. Optimum cycle efficiency versus cycle inlet temperature ratio of the two heat reservoirs and pressure ration.

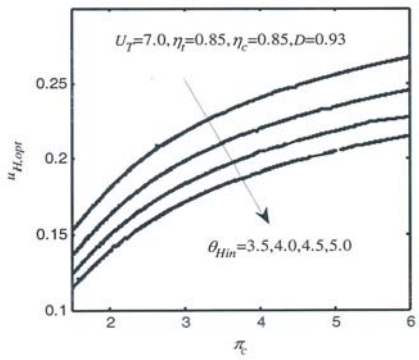

Figure 4. Optimum hot-side heat conductance distribution versus cycle inlet temperature ratio of the two heat reservoirs and pressure ration.

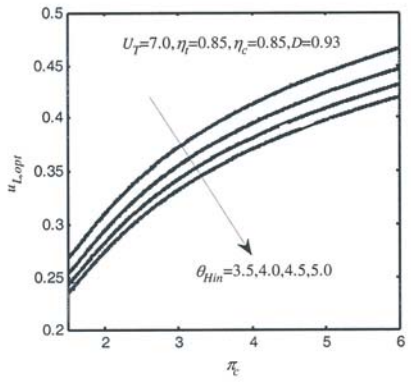

Figure 5. Optimum cold-side heat conductance distribution versus cycle inlet temperature ratio of the two heat reservoirs and pressure ration.

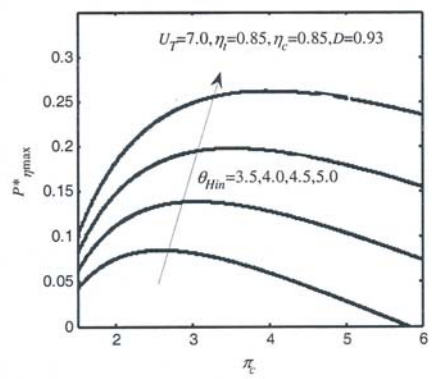

Figure 6. Corresponding dimensionless power under maximal dimensionless power versus cycle inlet temperature ratio of the two heat reservoirs and pressure ratio.

The influence of the total heat exchanger inventory (U_T) on the optimum cycle efficiency ($\eta_{\max}$) versus pressure ratio (π_c) with $\theta_{Hin} = 4.0$, $\eta_c = 0.85$, $\eta_t = 0.85$ and $D = 0.93$ is shown in Fig. 7. The corresponding optimum heat conductance distributions ($u_{H,opt}$ and $u_{L,opt}$) and dimensionless power under optimal cycle efficiency condition ($P^*_{\eta,\max}$) are shown in Figs. 8, 9 and 10.

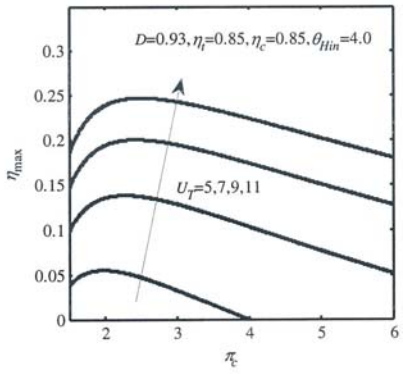

Figure 7. Optimum cycle efficiency versus heat exchanger inventory and pressure ratio.

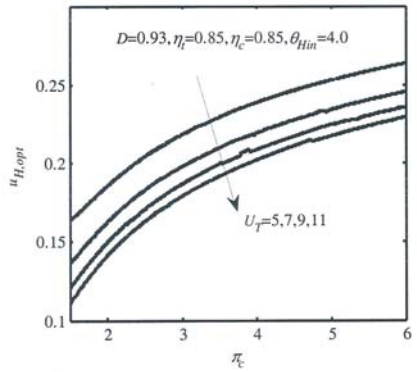

Figure 8. Optimum hot-side heat conductance distribution versus heat exchanger inventory and pressure ratio.

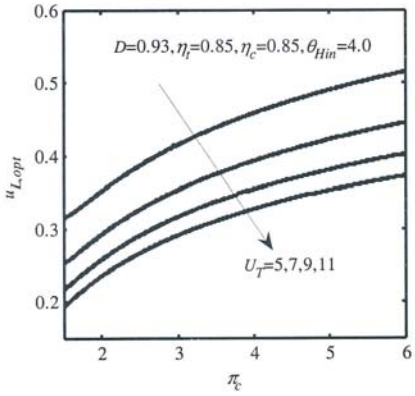

Figure 9. Optimum cold-side heat conductance distribution versus heat exchanger inventory and pressure ratio.

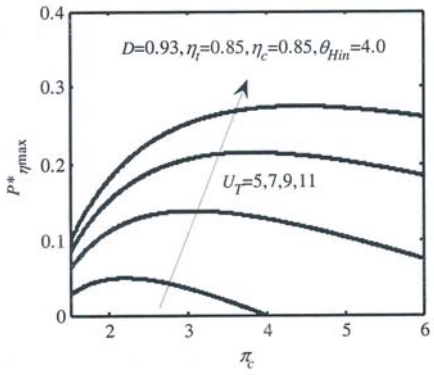

Figure 10. Corresponding dimensionless power under maximal dimensionless power versus heat exchanger inventory and pressure ratio.

The influence of the total pressure recovery coefficient (D) on the optimum cycle efficiency ($\eta_{\max}$) versus pressure ratio (π_c) with $\theta_{Hin} = 4.0$, $U_T = 7.0$ kW/K, $\eta_c = 0.85$ and $\eta_t = 0.85$ is shown in Fig. 11. The corresponding optimum heat conductance distributions ($u_{H,opt}$ and $u_{L,opt}$) and dimensionless power under optimal cycle efficiency condition ($P^*_{\eta,\max}$) are shown in Figs. 12, 13 and 14.

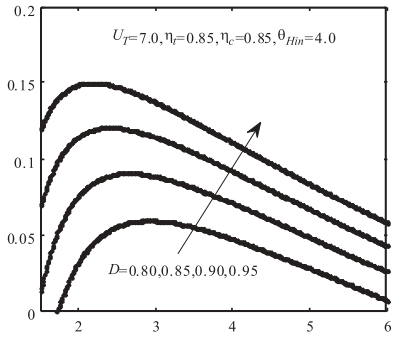

Figure 11. Optimum dimensionless power versus total pressure recovery coefficient and pressure ratio.

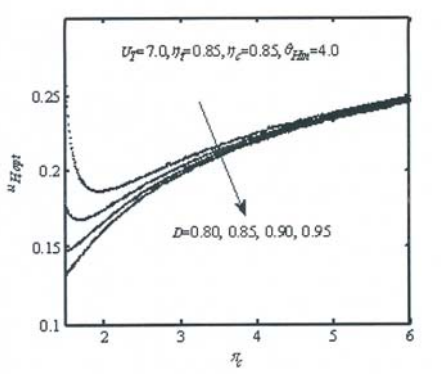

Figure 12. Optimum hot-side heat conductance distribution versus total pressure recovery coefficient and pressure ratio.

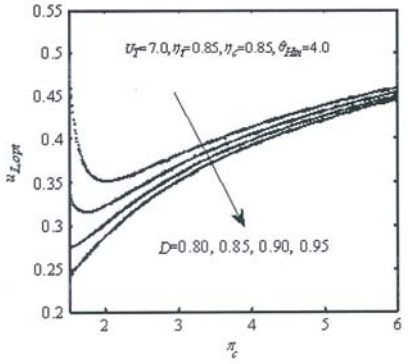

Figure 13. Optimum cold-side heat conductance distribution versus total pressure recovery coefficient and pressure ratio.

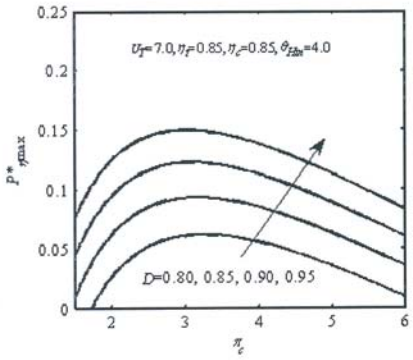

Figure 14. Corresponding cycle efficiency under maximal dimensionless power versus total pressure recovery coefficient.

These numerical results indicate that there exists a pair of optimum heat conductance distributions and an optimum pressure ratio corresponding to the double maximum cycle efficiency. For different pressure ratios, there exist different optimum heat conductance distributions corresponding to optimum cycle efficiency. In the power optimization results reported regarding the conventional internal combustion gas turbine cycles including the regenerated Brayton cycle [28–32] and the intercooled regenerated Brayton cycles

[33–38] in which the combustion process dominates the cycle performance, while regeneration of exhaust heat is a supplementary consideration to improve the total thermal efficiency, the optimum pressure ratio approaches the critical condition $u_H + u_L = 1$. However, with regard to IFGT cycles, the heat absorbed by the working air within the HTHE predominantly serves as the available energy source to drive the turbine. Therefore, the heat conductance ratio of the high temperature heat exchanger is always the highest of the three, a result that can be seen from optimization results. Such peculiar characteristics of the IFGT cycles should be seriously considered in the process of design and practical operational characteristics.

This aspect of the cycle is much different as compared to the conventional combustion gas turbine cycles [28] including the regenerated Brayton [29–33]. A close scrutiny of the performance behaviour further reveals the following interesting points during the design and development of IFGT cycles.

Both the optimum cycle efficiency $\eta_{\max}$ and the corresponding dimensionless power output $P^*_{\eta,\max}$ increase with the increases of the inlet temperature ratio of the two heat reservoirs θ_{Tin}, the total heat exchanger inventory U_T, and the total pressure recovery coefficient D. As well, both the optimum hot-side heat conductance distribution $u_{H,opt}$ and the optimum cold-side heat conductance distribution $u_{L,opt}$ increase with decreases of the inlet temperature ratio of the two heat reservoirs θ_{Tin}, the total heat exchanger inventory U_T , and the total pressure recovery coefficient D.

4 Conclusions

The performance of a closed indirectly-fired gas turbine cycle coupled to variable-temperature heat reservoirs with heat transfer irreversibility in the hot- and cold-side heat reservoirs and the high temperature heat exchanger, irreversible compression and expansion losses in the compressor and turbine, the pressure drop loss in the piping and the effect of the finite thermal capacity rate of the heat reservoirs are optimized by taking the power output as the optimization objective.

The optimization is performed by optimizing the distribution of the heat conductances between the hot- and cold-side heat reservoirs and the high temperature heat exchanger for a fixed total heat exchanger inventory. The impact of various parameters on the optimum power, optimum heat conductance ratios, and the corresponding cycle efficiency are analyzed.

The optimum distribution of heat conductance derived generally leads to a minimum heat exchanger inventory for a fixed power output. Therefore, the optimization carried out herein will lead to an indirectly-fired gas turbine power plant design with a smaller size and higher efficiency. The analysis and optimization may provide guidelines for the optimal design in terms of power, thermal efficiency and engine size for real closed IFGT power plants.

Acknowledgements This work is financially supported by the Qing-Lan Project of Jiangsu Province for universities' outstanding youth skeleton teachers under contract No. 161220605 and the Startup-grant of Jiangsu University of Science and Technology for academic research under contract No. 2005JD009J. The corresponding author also owes great thanks to School of Mechanical, Aerospace and Civil Engineering in the University of Manchester for providing excellent collaborative research facilities.

Received 19 June 2010

References

[1] Novikov I.I.: *The efficiency of atomic power stations*. Journal of Nuclear Energy **2**(1957), 7, 125–128.

[2] Chambadal P.: *Nuclear Power*. Armand Colin , Paris 1957.

[3] Curzon F.L., Ahlborn B.: *Efficiency of a Carnot engine at maximum power output*. American Journal of Physics **43**(1975), 1, 22–24.

[4] Bejan A.: *Entropy Generation Minimization*. CRC Press, New York 1996.

[5] Chen L., Sun F.: *Advances in Finite-time Thermodynamics*. Nova Science, New York 2004.

[6] Martinot E., Dienst C., Weiliang L.: *Renewable energy futures: Targets, scenarios, and pathways*. Annual Review of Environment and Resources **32**(2007), 1, 205–239.

[7] Athena P., Simon S., Paul U.: *Project ARBRE: Lessons for bio-energy developers and policy-makers*. Energy Policy **36(**2008), 6, 2044–2050.

[8] Salamon P., Hoffmann K.H., Schubert S.: *What conditions make minimum entropy production equivalent to maximum power production?* Journal of Non-equilibrium Thermodynamics **26**(2001), 1, 73–83.

[9] Klara J.M., Izsak M.S., Wherley M.R.: *Advanced power generation: The potential of indirectly-fired combined cycle*. ASME Paper 95-GT-261 (1995).

[10] Nelson J.O.: *High pressure ceramic air heater for indirectly-fired gas turbine applications*. Joint Contractors Review Meeting, DOE-METC, 1993

[11] Solomon P.R., Serio M.A., Cosgrove J.E.: *A coal-fired heat exchanger for an externally fired gas turbine*. Journal of Engineering for Gas Turbines and Power **118**(1996), 1, 23–31.

[12] DiCarlo J.A., van Roode M.: *Ceramic composite development for gas turbine engine hot section components*. In: Proceedings of ASME Turbo Expo 2006: Power for Land, Sea and Air, Barcelona 2006.

[13] Schulte-Fischedick J., Dreissigacker V., Tamme R.: *An innovative ceramic high temperature plate-fin heat exchanger for EFCC processes*. Applied Thermal Engineering **27**(2007), 8-9, 1285–1294.

[14] Aquaro D., Piccitto U., Pieve M.: *Feasibility analysis of a high temperature heat exchanger for combined cycles*. International Journal of Heat and Technology **21**(2003), 2, 167–174.

[15] Yan J., Eidensten L.: *Status and perspective of externally fired gas turbines*. Journal of Propulsion and Power **16**(2000), 4, 572–576.

[16] Bram S., de Ruyck J., Novak-Zdravkovic A.: *Status of external firing of biomass in gas turbines*. In: Proceedings of the Institution of Mechanical Engineers, Part A. Journal of Power and Energy **219**(2005), 2, 137–145.

[17] Martin K., Ulf H.: *The externally-fired gas-turbine (EFGT-Cycle) for decentralized use of biomass*. Applied Energy **84**(2007), 7-8, 795–805.

[18] Daniele C., Paolo D., Giorgio C.: *Performance evaluation of small size externally fired gas turbine(EFGT) power plants integrated with direct biomass dryers*. Energy **31**(2006), 10-11, 1459–1471.

[19] LaHaye P.G., M.R. Bary: *Externally fired combustion cycle (EFCC): A DOE clean coal V project: Effective means of rejuvenation for older coal-fired stations*. ASME Paper 94-GT-483 (1994).

[20] Consonni S., Macchi E., Farina F.: *Externally fired combined cycles (EFCC). Part A: thermodynamics and technological issues*. ASME Paper 96-GT-92 (1996).

[21] Consonni S., Macchi E.: *Externally fired combined cycles (EFCC). Part B: alternative configurations and cost projections*. ASME Paper 96-GT-93 (1996).

[22] Eidensten L., Yan J., Svedberg G.: *Biomass externally fired gas turbine cogeneration*. Journal of Engineering for Gas Turbines and Power **118**(1996), 3, 604–609.

[23] Ferreira S.B., Pilidis P.: *Comparison of externally fired and internal combustion gas turbines using biomass fuel*. Journal of Energy Resources **123**(2001), 4, 291–296.

[24] Koetzier H., Knoef H.: *Technical and economic feasibility of an indirectly fired gas turbine for rural electricity production from biomass*. Report No. 9712, EWAB Project, 1997.

[25] Evans R.L., Zaradic A.M.: *Optimization of a wood-waste-fuelled, indirectly fired gas turbine cogeneration plant*. Bioresource Technology **57**(1996), 2, 117–126.

[26] Bejan A., Tsatsaronis G., Moran M.: *Thermal Design & Optimization*. Wiley, New York 1996.

[27] Ferreira S.B., Pilidis P.: *Comparison of externally fired and internal combustion gas turbines using biomass fuel*. ASME Journal of Energy Resources Technology **123**(2001), 4, 291–296.

[28] Chen L., Sun F., Wu C.: *Theoretical analysis of the performance of a regenerated closed Brayton cycle with internal irreversibilities*. Energy Conversion and Management **18**(1997), 9, 871–877.

[29] Chen L., Ni N., Cheng G.: *FTT performance of a closed regenerated Brayton cycle coupled to variable temperature heat reservoirs*. In: Proc. Int. Conf. Marine Engng. 3.7.1–3.7.7, Shanghai, Nov. 4–8, 1996.

[30] Chen L., Ni N., Cheng G.: *Performance analysis for a real closed regenerated Brayton cycle via methods of finite time thermodynamics*. International Journal of Ambient Energy **20**(1999), 2, 95–104.

[31] Roco J., Veleasco S., Medina A.: *Optimum performance of a regenerative Brayton thermal cycle*. Journal of Applied Physics **82**(1997), 6, 2735–2741.

[32] Chen L., Sun F., Wu C.: *Power optimization of a regenerated closed variable-temperature heat reservoir Brayton cycle*. International Journal of Sustainable Energy **26**(2007), 1, 1–17.

[33] Chen L., Wang W., Sun F., Wu C.: *Closed intercooled regenerator Brayton cycle with constant-temperature heat reservoirs*. Applied Energy **77**(2004), 4, 429–446.

[34] Chen L., Wang W., Sun F., Wu C.: *Performance analysis for an irreversible closed variable-temperature heat reservoir intercooled regenerated Brayton cycle*. Energy Conversion and Management **44**(2003), 17, 2713–2732.

[35] Chen L., Wang W., Sun F.: *Power density analysis and optimization of an irreversible closed intercooled regenerated Brayton cycle*. Mathematical and Computer Modelling **48**(2008), 3-4, 527–540.

[36] Wang W., Chen L., Sun F., Wu C.: *Optimal heat conductance distribution and optimal intercooling pressure ratio for power optimisation of irreversible closed intercooled regenerated Brayton cycle*. Journal of the Energy Institute **79**(2006), 2, 116–119.

[37] Wang W., Chen L., Sun F., Wu C.: *Power optimization of an irreversible closed intercooled regenerated Brayton cycle coupled to variable-temperature heat reservoirs*. Applied Thermal Engineering **25**(2005), 8-9, 1097–1113.

[38] Wang W., Chen L., Sun F., Wu C.: *Performance analysis for an irreversible variable temperature heat reservoir closed intercooled regenerated Brayton cycle*. Energy Conversion and Management **44**(2003), 17, 2713–2732.